

Attribution-NonCommercial-NoDerivatives 4.0 International (CC BY-NC-ND 4.0)
<https://creativecommons.org/licenses/by-nc-nd/4.0/>

Access to this work was provided by the University of Maryland, Baltimore County (UMBC) ScholarWorks@UMBC digital repository on the Maryland Shared Open Access (MD-SOAR) platform.

Please provide feedback

Please support the ScholarWorks@UMBC repository by emailing scholarworks-group@umbc.edu and telling us what having access to this work means to you and why it's important to you. Thank you.



RESEARCH ARTICLE

10.1002/2017JA024385

Key Points:

- The annual number and duration of Alfvénic solar wind fluctuations (ALFs) varies by an order of magnitude over SC23
- There is an abrupt transition from ALFs being embedded in slow wind until 2002 to ALFs being dominantly in fast wind since 2003
- Substorm frequency increases by 40% from 2002 to 2003, simultaneous to increase of ALF activity

Correspondence to:

E. I. Tanskanen,
eija.tanskanen@aalto.fi

Citation:

Tanskanen, E. I., Snekvik, K., Slavin, J. A., Pérez-Suárez, D., Viljanen, A., Goldstein, M. L., ... Mursula, K. (2017). Solar cycle occurrence of Alfvénic fluctuations and related geo-efficiency. *Journal of Geophysical Research: Space Physics*, 122, 9848–9857. <https://doi.org/10.1002/2017JA024385>

Received 22 MAY 2017

Accepted 26 SEP 2017

Accepted article online 3 OCT 2017

Published online 17 OCT 2017

©2017. The Authors.

This is an open access article under the terms of the Creative Commons Attribution-NonCommercial-NoDerivs License, which permits use and distribution in any medium, provided the original work is properly cited, the use is non-commercial and no modifications or adaptations are made.

Solar Cycle Occurrence of Alfvénic Fluctuations and Related Geo-Efficiency

E. I. Tanskanen¹ , K. Snekvik² , J. A. Slavin³ , D. Pérez-Suárez⁴ , A. Viljanen⁵,
M. L. Goldstein⁶ , M. J. Käpylä^{1,7} , R. Hynönen¹ , L. V. T. Häkkinen⁵ , and K. Mursula⁸
¹ReSoLVE Centre of Excellence, Aalto University, Espoo, Finland, ²Birkeland Centre for Space Sciences, University of Bergen, Bergen, Norway, ³Department of Climate and Space Sciences and Engineering, University of Michigan, Ann Arbor, MI, USA, ⁴University College London, UK, ⁵Finnish Meteorological Institute, Helsinki, Finland, ⁶Space Science Institute, Boulder, CO, USA, ⁷Max Planck Institute for Solar System Research, Göttingen, Germany, ⁸Space Climate Research Unit, ReSoLVE Centre of Excellence, Oulu University, Oulu, Finland

Abstract We examine solar wind intervals with Alfvénic fluctuations (ALFs) in 1995–2011. The annual number, the total annual duration, and the average length of ALFs vary over the solar cycle, having a maximum in 2003 and a minimum in 2009. ALFs are most frequent in the declining phase of solar cycle, when the number of high-speed streams at the Earth's vicinity is increased. There is a rapid transition after the maximum of solar cycle 23 from ALFs being mainly embedded in slow solar wind (<400 km/s) until 2002 to ALFs being dominantly in fast solar wind (>600 km/s) since 2003. Cross helicity increased by 30% from 2002 to 2003 and maximized typically 4–6 h before solar wind speed maximum. Cross helicity remained elevated for several days for highly Alfvénic non-ICME streams, but only for a few hours for ICMEs. The number of substorms increased by about 40% from 2002 to 2003, and the annual number of substorms closely follows the annual cross helicity. This further emphasizes the role of Alfvénic fluctuations in modulating substorm activity. The predictability of substorm frequency and size would be greatly improved by monitoring solar wind Alfvénic fluctuations in addition to the mean values of the important solar wind parameters.

1. Introduction

The existence of Alfvén waves was predicted in 1942 by Hannes Alfvén (Alfvén, 1942). It is known since then that Alfvén waves occur in the magnetosphere (Cummings, O'Sullivan, & Coleman, 1969) and in the solar wind (SW) (Coleman, 1968). Moreover, a few years ago, Alfvén waves were also observed in the solar corona (Banerjee, Pérez-Suárez, & Doyle, 2009; McIntosh et al., 2011), where they may have an important role in accelerating the solar wind.

The connection between solar activity and geomagnetic activity was recognized already in 1859 during the famous Carrington storm (Carrington, 1859). The two main forms of geomagnetic activity are geomagnetic storms and substorms (Birkeland, 1908; Chree, 1912), which are measured by equatorial and high-latitude magnetometers, respectively. The occurrence of storms peaks at solar maximum (Chapman & Ferraro, 1930), while the number of substorms peaks a few years later in the declining phase of the solar cycle (Tanskanen et al., 2002; Tanskanen et al., 2011). Substorms occur daily (Akasofu & Chapman, 1961; Kallio et al., 2000; Kullen & Karlsson, 2004), while medium-sized or larger geomagnetic storms occur typically once per month (Häkkinen et al., 2003; Yakovchouk et al., 2012).

The main solar wind drivers of geomagnetic activity are interplanetary coronal mass ejections (ICME) and high-speed streams (HSS) together with corotating interaction regions (CIR) (Richardson & Cane, 2012; Sawyer & Haurwitz, 1976; Tanskanen et al., 2005; Zhang et al., 2007). However, the relationship of HSSs and ICMEs to geomagnetic activity at different latitudes, as well as their occurrence over the solar cycle, varies considerably (Holappa et al., 2014; Holappa, Mursula, & Asikainen, 2014).

The magnitude and direction of the B_z component of the interplanetary magnetic field (IMF) is known to be the most important factor controlling energy transfer from the solar wind into the Earth's magnetosphere (Fairfield & Cahill, 1966). Energy input from the solar wind into the magnetosphere increases as the IMF becomes increasingly antiparallel to the equatorial geomagnetic field (i.e., southward oriented). It is primarily during structures such as large magnetic flux ropes and magnetic clouds of ICMEs when the IMF may attain a

long interval of strongly southward orientation (Burlaga et al., 1982), which is required to produce intense storms in the Earth's magnetosphere (Holzer & Slavin, 1981).

Alfvénic waves in the solar wind, on the other hand, can produce repeated periods of weakly negative IMF, typically between -1 and -10 nT. Several papers suggest that Alfvénic waves within the corotating streams enhance substorm activity (D'Amicis, Bruno, & Bavassano, 2007; McPherron, Weygand, & Hsu, 2008; Tsurutani et al., 1990; Tsurutani et al., 1995), power HILDCAAs (high-intensity long-duration continuous AE activity; Tsurutani & Gonzalez, 1987), and contribute to ring current formation (Søråas et al., 2004). D'Amicis, Bruno, and Bavassaro (2011) and D'Amicis and Bruno (2015) found out that solar wind fluctuations during the maximum phase of solar cycle 23 (SC23) are highly Alfvénic. Roberts and Goldstein (1990) reported that Alfvénic intervals often accompany large and extended auroral activity, although the reverse was not found to be true. They examined intervals around the maximum of solar cycle when the interplanetary Alfvén waves and their effects to geomagnetic activity are more often due to the slow solar wind (Chian et al., 2006; D'Amicis et al., 2007; Gonzalez, Clúa de Gonzalez, & Tsurutani, 1995).

In this paper, we study solar wind Alfvénic fluctuations (ALFs), in particular their occurrence in 1995–2011 and relation to high-latitude geomagnetic activity. Earlier studies on the same topic had more limited time range and did not cover a full solar cycle. We calculate the annual number and total duration of ALFs, as well as their mean cross helicity. We study how cross helicity is distributed in time for ALFs within ICME-related solar wind and highly and weakly Alfvénic not-ICME-related solar wind. We also calculate the annual occurrence of ALFs within fast and slow solar wind separately and examine how the number of substorms and storms vary during the time interval 1995–2011.

2. Data and Methods

We have developed data mining tools to find Alfvénic fluctuations and high-speed streams (with a code called HSSeeker) and to determine storm and substorm occurrence rates (SSeeker; Tanskanen et al., 2005) in order to compare the different solar wind structures (ICME, HSS, slow wind) and ALFs related to these structures with different forms of space weather in the Earth's magnetosphere. The initial search for solar wind streams was done using the 5 min data of the OMNI-2 database (King and Papitashvili, 2005), as explained in Snekvik, Tanskanen, and Kilpua (2013). However, the helicity analysis was done using original measurements by the WIND and ACE spacecraft in order to preserve the spectral properties of the IMF, which may be modified in the OMNI data due to the shift of the data from the site of observation to the bow shock of the Earth's magnetosphere. For the WIND spacecraft, we used the 92 s data of the SWE plasma instrument (Ogilvie et al., 1995) and the 3 s version of magnetic field data of the MFI instrument (Lepping et al., 1995). For the ACE satellite, we used the 64 s Level 2 proton data of SWEPAM instrument (McComas et al., 1998) and the 16 s Level 2 magnetic field data of MAG instrument (Smith et al., 1998). The higher-sampling magnetic data were median averaged to the lower sampling frequency of the plasma data of the respective satellite. We used WIND and ACE data alternately, selecting the data of that satellite that had a more complete data set (less data gaps) available for any 512-point averaging interval. Note also that, because of the long 512-point averaging interval, no practical difference in results was found between the slightly differently sampled WIND and ACE data.

The cross helicity

$$H_c = \langle \mathbf{v}' \cdot \mathbf{v}_A' \rangle \quad (1)$$

is a measure of the correlation between the fluctuations of solar wind velocity and Alfvén velocity (\mathbf{v}' and \mathbf{v}_A' , respectively). (The mean is denoted by $\langle \rangle$ and taken here over a sample interval of 512 data points.) Solar wind ALFs are identified by the normalized cross helicity (Snekvik et al., 2013; Tu & Marsch, 1995)

$$\sigma_c = \frac{2\langle \mathbf{v}' \cdot \mathbf{v}_A' \rangle}{\langle v'^2 \rangle + \langle v_A'^2 \rangle} = \frac{\text{Var}(Z_{\text{out}}) - \text{Var}(Z_{\text{in}})}{\text{Var}(Z_{\text{out}}) + \text{Var}(Z_{\text{in}})} \quad (2)$$

where Var means the variance of $Z_{\text{out}} = \mathbf{v}' - \mathbf{v}_A'$ and $Z_{\text{in}} = \mathbf{v}' + \mathbf{v}_A'$, the two Elsässer variables denoting the outward and inward propagating Alfvén waves for an outward oriented IMF, respectively (for more information, see Tu & Marsch, 1995; Snekvik et al., 2013). For inward IMF the signs are interchanged, that is,

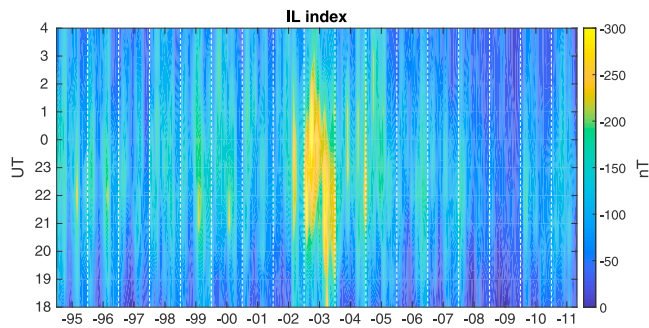


Figure 1. High-latitude geomagnetic activity based on IL, the westward electrojet index in Scandinavian sector in 1995–2011. Amplitude of IL index (in nT) is color-coded such that the largest monthly disturbances are shown by yellow and smallest by blue.

We use here ground-based magnetic field measurements from the high-latitude IMAGE network (Tanskanen, 2009) in Fenno-Scandinavia in 1995–2011. We identify substorms from the westward electrojet index, IL index (Kallio et al., 2000), constructed from IMAGE data. Figure 1 depicts the IL index (in nT) in 1995–2011 at monthly resolution (for separate UT hour), color-coded so that blue shows the smallest activity and yellow the largest activity. Only the time interval between 18 and 04 UT is shown, when the IL magnetometers are located around the midnight, where substorms occur. Figure 1 shows that the largest high-latitude geomagnetic activity is observed during the early declining phase of SC23 with a rapid increase in late 2002 and a decrease after 2003. Geomagnetic storms are identified from the geomagnetic *Dst* index (Sugiura, 1964). A storm is in progress when the *Dst* is below -50 nT.

3. Annual Number and Duration of ALFs

Figure 2 shows the ALF occurrence rate, that is, the annual ALF numbers in 1995–2011, covering the whole solar cycle 23. ALFs are observed in each year, but there is a large variation over the solar cycle. There is a high ALF number period of more than 60 ALFs per year from 1999 to 2005, with a maximum ALF number in 2003, when more than 100 ALFs are observed (roughly eight per solar rotation). The smallest number of ALFs is found at sunspot minimum in 2009, when only 10 ALFs occurred in the entire year. Accordingly, the number of ALFs varies roughly by 1 order of magnitude during SC23.

Figure 2 also depicts the total annual duration of ALF intervals in days. In 2003 the ALF activity covered 189 days, that is, more than half a year. Taking into account the fact that there are some gaps in the data (as discussed above), this is an impressive coverage. Annual ALF duration was roughly 3 times longer for ALF active years (ALF number > 60) than for less active years (ALF number < 60). In 2009 the total ALF activity covered only 7 days. Comparing to the year 2003, this implies that the solar cycle variation in annual ALF duration was even relatively larger than in ALF occurrence. This also suggests that there is a solar cycle variation in the (annually averaged) mean length of ALFs so that a typical ALF is somewhat longer in the ALF active years than in less active years.

Next we divided the ALFs into two categories: slow solar wind (SW) ALFs if the mean speed during the ALF is at most 400 km/s and fast solar wind ALFs if the solar wind speed during the ALF equals or exceeds 600 km/s. Figure 3 shows the annual number of fast and slow solar wind ALFs separately. The occurrence rate of slow solar wind ALFs increases fairly systematically from the previous solar minimum to a maximum in 2002, but then declines rapidly in 2003. On the other hand, the number of fast SW ALFs remains rather small until 2002, clearly below the number of slow SW

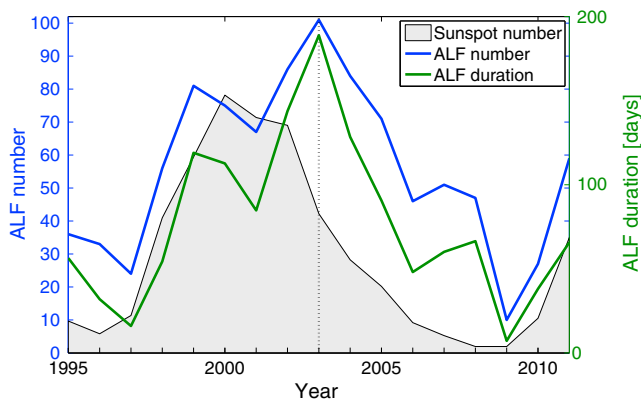


Figure 2. Yearly number of Alfvénic fluctuations in 1995–2011 (blue line) and yearly total ALF duration in days (green line; right y axis). Sunspot numbers are shown as a gray shaded area for reference. Year 2003 is marked by a dotted vertical line.

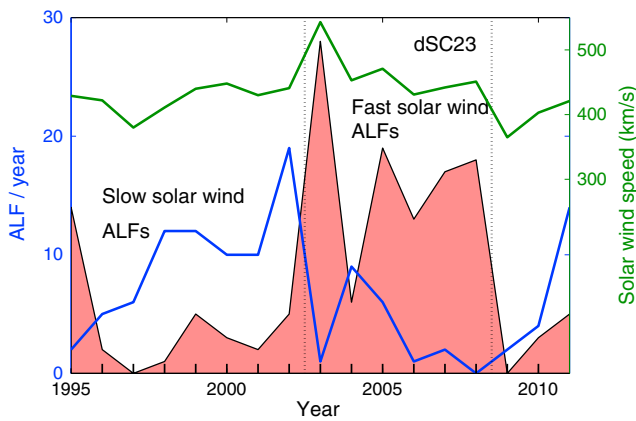


Figure 3. Yearly number of ALFs (left y axis) within slow (<400 km/s) solar wind (blue line) and within fast (≥ 600 km/s) solar wind (black line with pink shaded area) in 1995–2011. Yearly means of solar wind speed (right y axis) are denoted by a green line. Declining phase of SC23 and dSC23 is marked by dotted vertical lines.

ALFs, but then rapidly increases to a maximum in 2003. The number of fast SW ALFs remains quite high until 2008, far higher than the number of slow SW ALFs.

These results show a rapid transition in the properties of solar wind speed carrying ALFs when turning from the solar cycle maximum to the declining phase of the SC23. Figure 3 also includes the annual means of solar wind speed, showing that the annual solar wind speed increased from 440 km/s in 2002 to 540 km/s in 2003. It is known that HSSs dominated most of the year 2003 (Mursula, Lukianova, & Holappa, 2015; Tanskanen et al., 2005), and the solar wind speed was exceptionally high, especially during the solstice months (Mursula, Holappa, & Lukianova, 2017). Accordingly, the rapid increase of the mean solar wind speed from 2002 to 2003 is manifested as a rapid decline of ALFs carried by the slow solar wind and an increase of ALFs carried by the fast solar wind.

4. Annual Cross Helicity of ALFs

Figure 4a shows the yearly averaged cross helicity of all ALFs of the year. Note that for the cross helicity to attain a large value, both the ALF amplitude (denominator of equation (2)) and alignment (normalized cross helicity, equation (1)) have to be large. Yearly averaged cross helicity varies from the minimum of less than $500 \text{ km}^2/\text{s}^2$ in 1997 (solar minimum year between SC22 and SC23) to the maximum of about $2,000 \text{ km}^2/\text{s}^2$ in 2003. During the minimum between SC23 and SC24 cross helicity reached another deep local minimum, at a slightly higher level than during the previous minimum. Note that the mean cross helicity in 2000, during the maximum of SC23, is only 30% larger than during the next solar minimum and reaches only 60% of the maximum value in 2003. The yearly mean values exceeding $1,400 \text{ km}^2/\text{s}^2$ (dotted horizontal line in Figure 4a) are only seen during the declining phase in 2002–2003 and 2005–2008.

The yearly averaged solar wind speed during ALFs is depicted in Figure 4b. One can see that the yearly mean ALF solar wind speed increases from 2002 to 2003 by almost the same percentage as the full annual means of solar wind speed (see Figure 3), but the ALF speeds are slightly higher than the mean speeds, due to the selection effect of ALFs. However, the ALF solar wind speed attains only a local maximum in 2003, and somewhat higher values of up to 600 km/s are found during the late declining phase in 2005–2008, with a maximum in 2008. This seemingly surprising result is due to the fact that, as Figures 2 and 3 show, there are some 50 (about 65%) intermediate-speed ALFs ($400 \text{ km/s} < v < 600 \text{ km/s}$) in 2003 but only some 15 (45%) in 2006–2008. Moreover, the relative fraction of slow wind ALFs is decreasing from 2005 to a minimum in 2008, leading to a maximum in Figure 4b in 2008.

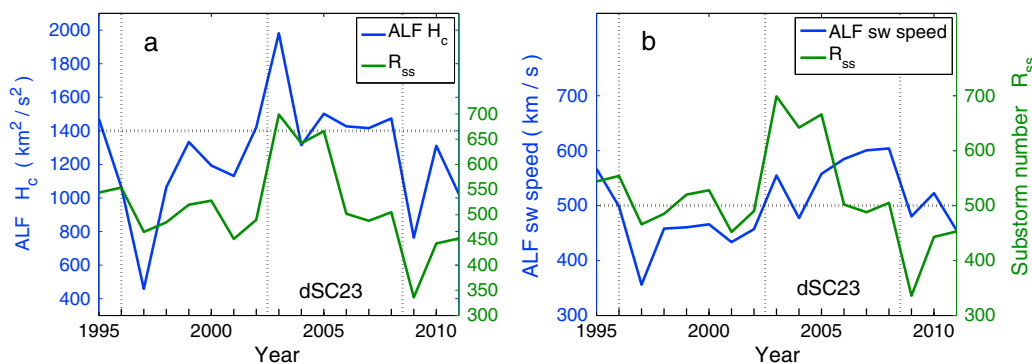


Figure 4. Yearly averaged (a) cross helicity of ALFs (blue curve, left y axis) and (b) solar wind speed during ALF intervals (blue curve, left y axis) in 1995–2011. Yearly averaged substorm number R_{ss} is included in both panels (green curve, right y axis). Declining phases of SC22 and SC23 and dSC23 are marked by dotted vertical lines.

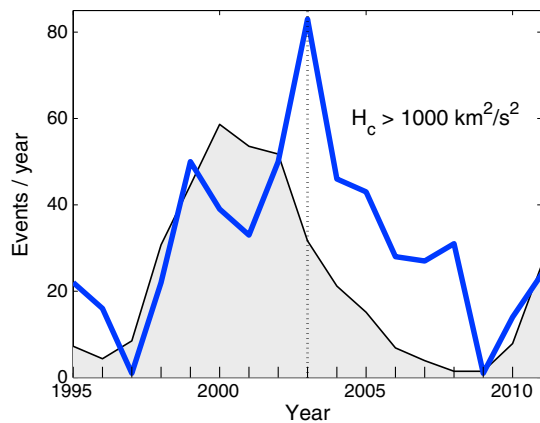


Figure 5. Yearly number of ALFs with cross helicity $H_c > 1,000 \text{ km}^2/\text{s}^2$ (blue line). Sunspot numbers are shown as a gray shaded area for reference. Year 2003 is marked by a dotted vertical line.

ALFs have a cross helicity larger than $1,000 \text{ km}^2/\text{s}^2$. On the other hand, in 2009, the large-cross helicity ALFs practically vanish. Thus, the solar cycle variation of large-cross helicity ALFs is relatively even larger than for ALF number or duration.

5. ALFs Embedded Within Different Solar Wind Structures

Alfvénic fluctuations can appear in both slow and fast speed streams as well as ICMEs (Roberts et al., 1987; Snekvik, 2013). We used here the division of solar wind to these three solar wind structures (partly also unspecified solar wind), based on 5 min OMNI data, median filtered over 10 h (for more details, see Snekvik et al., 2013). We calculated the cross helicities and normalized cross helicities for ICMEs and non-ICME structures. The latter were further divided into two classes: the highly Alfvénic streams (high ALFs) and weakly Alfvénic streams (weak ALFs) according to the mean value of $\sigma_c \geq 0.8$ or $\sigma_c < 0.8$ during the stream, respectively. The highly Alfvénic streams are a part of ALFs discussed above, but the weakly Alfvénic streams are a new class outside the ALF definition adopted above. Note that, although a considerable amount of ICMEs are included within ALFs (as defined and studied above), there are also several ICMEs that are not ALFs (i.e., do not have $\sigma_c > 0.8$).

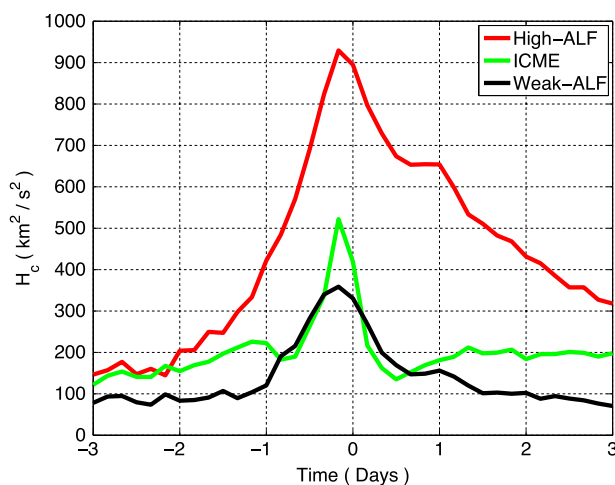


Figure 6. Superimposed epoch plot of cross helicity for high ALF (red curve), ICMEs (green curve), and weak ALFs (black curve) from 3 days before to 3 days after the zero epoch time (maximum solar wind speed).

Both panels of Figure 4 show the annual numbers of substorms, which follow fairly reliably the evolution of the mean annual cross helicity (Figure 4a). Accordingly, the correlation between the substorm number and cross helicity is very good (Pearson correlation coefficient $r = 0.7$, probability of random correlation $p = 0.004$). On the other hand, correlation between the substorm number and mean ALF speed remains insignificant ($r = 0.3$, $p = 0.22$) because of the above discussed maximum in the late declining phase of SC23 in ALF mean speed.

The annual number of those ALFs whose cross helicity H_c is larger than $1,000 \text{ km}^2/\text{s}^2$ is shown in Figure 5. These form the part of ALFs (for which $\sigma_c \geq 0.8$) where the amplitude of the fluctuations of the solar wind velocity and magnetic field is largest. Figure 5 shows a roughly similar solar cycle variation as depicted by the mean ALF cross helicity in Figure 4a. However, the maximum in 2003 is further emphasized, especially with respect to the situation in the later declining phase of the cycle. In 2003 more than 80% of

We have made a superposed epoch (SPE) analysis (Brier & Bradley, 1964) for the cross helicity H_c separately for ICMEs and non-ICMEs (high ALF and weak ALF). The SPE-curve was computed from 3 days before to 3 days after the maximum speed of the stream, which was selected as the superposed zero time ($t = 0$). Figure 6 depicts the superposed values of the cross helicity for high-ALF streams (red curve), ICMEs (green curve), and weak-ALF streams (black curve). Interestingly, the cross helicity is found to maximize several (typically 4–6) hours before the velocity maximum for all three solar wind structures. This means that the time evolution of cross helicity within the compression region before the solar wind speed maximum is quite similar for high-ALF, weak-ALF, and ICME-related structures.

The peak magnitude of SPE cross helicity for weakly Alfvénic streams ($358 \text{ km}^2/\text{s}^2$) is, as expected, much lower than the corresponding peak for the highly Alfvénic streams ($929 \text{ km}^2/\text{s}^2$). More interestingly, the peak SPE cross helicity of ICMEs ($521 \text{ km}^2/\text{s}^2$) is only 56% of the peak of the highly Alfvénic streams but still notably higher than for weak-ALF streams. The cross helicity SPE curve for ICMEs is also more limited around zero time than for either of the

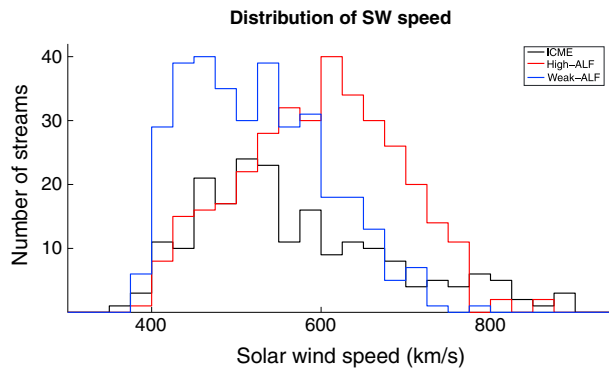


Figure 7. Distribution of solar wind speed during highly Alfvénic solar wind streams (high ALF), weakly Alfvénic solar wind streams (weak ALF), and interplanetary coronal mass ejections (ICME).

two other ALF groups. The interval of elevated SPE cross helicity lasts for several days for high ALFs, but only for a few hours for ICMEs and weak-ALF streams. The average cross helicity over the whole 6 day SPE interval for ICMEs is $203 \text{ km}^2/\text{s}^2$, for high ALFs $450 \text{ km}^2/\text{s}^2$, and for low ALFs $140 \text{ km}^2/\text{s}^2$. Thus, the average cross helicity for ICMEs is less than half of the average cross helicity for high ALFs and only somewhat larger than for weak ALFs.

The distribution of solar wind speed during the three structures is shown in Figure 7. One can see that about 50% of highly Alfvénic streams have a speed of $\geq 600 \text{ km/s}$ and could be classified among high-speed streams. On the other hand, only 18% of weakly Alfvénic streams belong to HSS category. Instead, about 44% of weakly Alfvénic streams have a slow speed of $\leq 450 \text{ km/s}$. Therefore, one can roughly equate the highly Alfvénic streams as high-speed streams and the weakly Alfvénic streams as slow-speed streams. The solar wind speed during ICMEs varies more

than during the two other streams. About 35% of ICMEs belong to the high-speed category, while 30% have a slow speed of $\leq 450 \text{ km/s}$. The mean speed of ICMEs is as high as 582 km/s , due to the long tail of the speed distribution (see Figure 7).

These results show that high-speed streams, which also cause most of substorms and high-latitude activity (Tanskanen et al., 2005; Holappa et al., 2014a), include typically somewhat larger cross helicities than ICMEs, which are mainly responsible for intense magnetic storms and low-latitude geomagnetic activity.

6. Annual Numbers of ICMEs, HSSs, Storms, and Substorms

We examine now the annual occurrence rate of substorms and storms and their two most important solar wind drivers, the ICMEs and HSS/CIRs, over the solar cycle 23. Figure 8 depicts the annual numbers of substorms (R_{ss}), storms (R_{st}), HSSs, and ICMEs in 1997–2010. (Yearly sunspot numbers, denoted by gray shaded

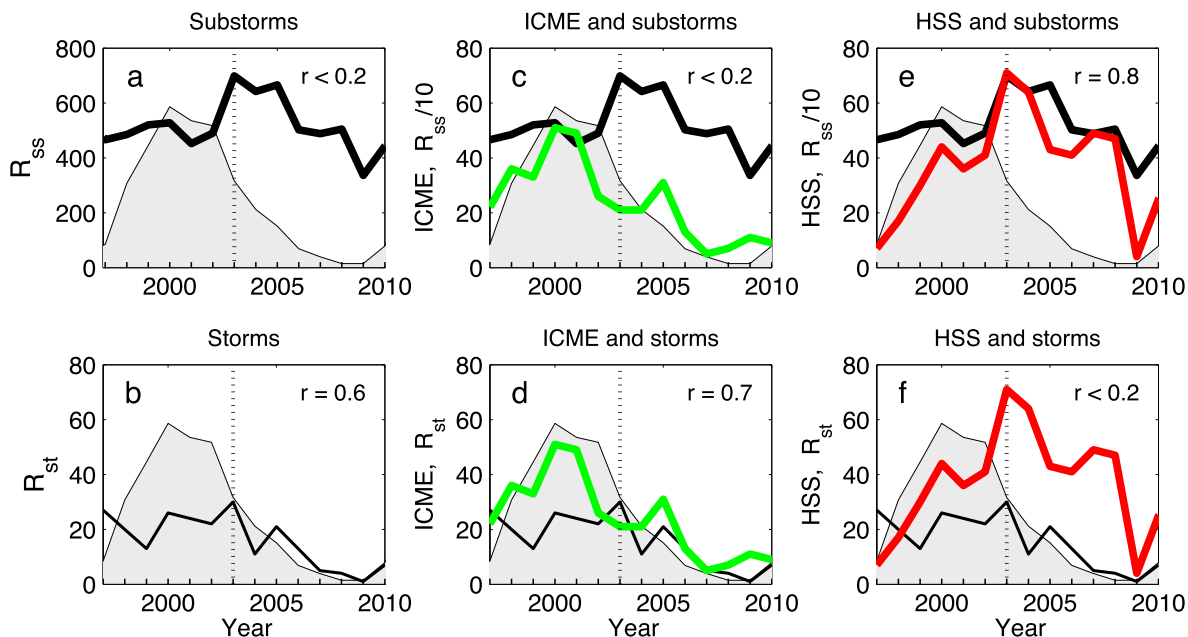


Figure 8. Yearly averaged numbers of geomagnetic storms and substorms and their main drivers (ICMEs and HSSs). Yearly averaged sunspot number (gray shaded area) is included in all panels for reference. (a) Yearly substorm number R_{ss} (thick black curve); (b) yearly storm number R_{st} (thin black curve); (c) R_{ss} and yearly occurrence of ICMEs (green curve); (d) R_{st} and yearly occurrence of ICMEs (green curve); (e) R_{ss} and yearly occurrence of HSSs (red curve); (f) R_{st} and yearly occurrence of HSSs (red curve). Linear correlation coefficients r between the two lines (Figures 8c–8f) or sunspots and the line (Figures 8a and 8b) are shown in the upper right corner of each panel. Year 2003 is marked by a dotted vertical line in each panel.

areas, are included in each panel for reference.) Storm numbers R_{st} are depicted in Figures 8b, 8d, and 8f, and the largest number of storms is found in 2003. The storm numbers of more than 20 storms in a year are found in 1997, 2000–2003, and in 2005.

Annual substorm numbers are depicted in Figures 8a, 8c, and 8e. (Note that substorm numbers used here are based on IMAGE magnetometers, which can reliably detect substorms in the 16–02 UT (18–04 LT) sector, when the IMAGE magnetometers are located at the nightside.) Substorms occur at a fairly similar frequency of about 450–500/year in the ascending phase over the solar maximum until 2002, and again in the later declining phase from 2006 to 2008. The highest frequency of substorms is detected in 2003–2005, when the substorm number exceeded 600/year. Year 2003 marks the maximum of substorm occurrence with 699 substorms, while in 2009, substorm occurrence was clearly lower than in any other year of SC23. Note that although year 2003 marked the maximum occurrence of both storms and substorms, the distribution of storms and substorms over the solar cycle 23 was clearly different. A large majority of storms occurred before 2003 but most substorms only thereafter.

The highest annual occurrence rates of ICMEs (Cane & Richardson, 2003; Kilpua et al., 2012; Richardson & Cane, 2012) (green curve in Figures 8c and 8d) are observed during the sunspot maximum in 2000–2001. Yearly, ICME numbers correlate very well with the sunspot numbers (correlation coefficient $r = 0.8$, $p = 0.0002$, not shown in Figure 8), in agreement with the fact that ICMEs are related to magnetic structures like prominences originating from active regions of the Sun. The correlation between storm numbers and ICME numbers is also highly significant ($r = 0.7$, $p = 0.004$), but the correlation between the substorm numbers and ICMEs is insignificant ($r = 0.2$, $p = 0.5$). On the other hand, the number of substorms and high-speed streams (red curve in Figures 8e and 8f) correlates very well ($r = 0.8$, $p = 0.0004$), supporting the earlier result that substorms are mainly driven by high-speed streams (Richardson & Cane, 2012; Tanskanen et al., 2005). However, storm numbers and high-speed streams do not vary similarly over the solar cycle ($r = 0.2$, $p = 0.5$).

7. Discussion

Interplanetary Alfvén waves with magnetic field fluctuations including periods of southward IMF are known to be important in increasing the dayside reconnection rate and enhancing geomagnetic activity especially at high latitudes (D'Amicis et al., 2006; D'Amicis et al., 2007, 2011; Hsu & McPherron, 2002; Tsurutani et al., 1990; Tsurutani & Gonzalez, 1987). The importance of the IMF southward component for geomagnetic activity was discovered as early as mid-1960s (Fairfield & Cahill, 1966). Tsurutani et al. (1990) examined the connection between Alfvén waves and substorm activity in 1979 and Lee et al. (2006) the effect of northward turnings of IMF B_z during Alfvénic intervals in 1996–2002.

Tsurutani and Gonzalez (1987) found that large-amplitude Alfvén waves occurred in the trailing portions of high-speed solar wind streams and that Alfvén waves were present during HILDCAA events. D'Amicis et al. (2007) reported that Alfvénic fluctuations were particularly geoeffective in 1995 (in the late declining phase of SC22), while they were less geoeffective during solar maximum. Previous studies on Alfvénic fluctuations have concentrated on examining rather short time intervals or earlier times (D'Amicis et al., 2007; Tsurutani et al., 1995).

In this paper we have examined the properties of Alfvénic fluctuations and their relation to geomagnetic activity in 1995–2011, covering well the full solar cycle 23. We have determined the yearly numbers and durations of Alfvénic fluctuations (see Figure 2) and the ALF-related solar wind speed (see Figure 4b) over the solar cycle, as well as the annual numbers of substorms and storms (see Figure 8). Alfvénic fluctuations are found throughout the solar cycle (Snekvik et al., 2013), but they clearly maximize in the year 2003, during the declining phase of SC23.

We found a rapid increase in yearly averaged ALF cross helicity during the early declining phase of the SC23, when the yearly averaged cross helicity increased by roughly 30% from 2002 to 2003 (see Figure 4a). Even thereafter, the ALF cross helicity was enhanced practically during the entire declining phase of SC23 until (and including) 2008. The change from 2002 to 2003 was examined in more detail by dividing the ALFs based on the related solar wind speed. The slow solar wind ALFs (speed < 400 km/s) dominated during the ascending phase and solar maximum of SC23 until 2002, while the fast ALFs (speed ≥ 600 km/s) started dominating abruptly in 2003 and dominated the declining phase of both SC23 and SC22. This rapid change from 2002 to

2003 is suggested to be due to the simultaneous increase in the mean solar wind, as more and more of HSSs started appearing at this time due to the development of both polar and low-latitude coronal holes (Mursula et al., 2015, 2017). The sharp increase in fast solar wind ALFs coincided with the increase of substorm intensity and number.

We have also studied here the Alfvénic properties of three different solar wind structures: ICMEs, as well as highly Alfvénic ($\sigma_c \geq 0.8$) and weakly Alfvénic ($\sigma_c < 0.8$) non-ICME streams. We showed that the highly Alfvénic (non-ICME) streams typically have a fairly high solar wind speed, and a large fraction could be classified as HSSs with speed faster than 600 km/s. On the other hand, the weakly Alfvénic streams typically have clearly slower speeds, although a fraction of HSSs are also rather weakly Alfvénic (i.e., have a small σ_c). Interestingly, the ICMEs have a very wide and flat distribution of solar wind speeds, including roughly one third of typically HSS speeds with a very long tail of speeds above 600 km/s and one third of slow speeds below 450 km/s.

The distribution of cross helicity within the three solar wind structures was studied using the superposed epoch analysis. The SPE peak cross helicity for the highly Alfvénic streams was found to be about $930 \text{ km}^2/\text{s}^2$, while for ICMEs it was about $520 \text{ km}^2/\text{s}^2$. For average SPE cross helicities the relative difference between high-ALF streams and ICMEs was even larger ($450 \text{ km}^2/\text{s}^2$ and $203 \text{ km}^2/\text{s}^2$, respectively). These results agree with the earlier observations reported by Belcher and Davis (1971), who showed, based on Mariner 5 data in 1967, that the most Alfvénic solar wind is observed during the high-speed streams.

We also found that cross helicity stays enhanced for several days after the peak for highly Alfvénic streams but drops sharply only few hours after the peak for ICMEs. This indicates that the HSS-related solar wind includes a considerably larger total amount of Alfvénicity than ICME-related solar wind. These results suggest that the role of Alfvénic fluctuations in modulating substorm activity is larger during HSSs than during ICME-related solar wind. The predictability of substorm frequency and size may be improved by monitoring the solar wind Alfvénic fluctuations in addition to the mean values of solar wind speed and magnetic field.

8. Main Results and Conclusions

We have shown that the characteristics of Alfvénic fluctuations in solar wind abruptly changed when the solar maximum of cycle 23 turned into the declining phase. While until 2002 the Alfvénic ($\sigma_c \geq 0.8$) intervals were mainly found in slow solar wind, from 2003 onward, they were dominantly found in high-speed streams. The yearly averaged cross helicity increased by 30% from 2002 to 2003. These abrupt changes are related to the increase of the yearly averaged solar wind speed from about 440 km/s in 2002 to 540 km/s in 2003 and, in particular, to the increasing number of high-speed streams within the solar wind.

Overall, the number of Alfvénic intervals varies roughly by 1 order of magnitude during SC23 from maximum of about 100 in 2003 to a minimum of 10 per year in 2009. The total annual duration of ALFs varies from more than 50% of time in 2003 to only 7 days in 2009. The solar cycle variation is relatively larger in ALF duration than in ALF occurrence, implying a solar cycle variation also in the average ALF length. ALFs are typically somewhat longer in the ALF active years than in less active years. Solar cycle variation is even larger in those ALFs that have higher than average cross helicity.

Cross helicity maximizes typically 4–6 h before the solar wind speed maximum, irrespective of solar wind structure. For ICMEs the peak superposed cross helicity was roughly half of high-ALF streams and only somewhat higher than for weakly Alfvénic streams. Moreover, the interval of elevated cross helicity lasts for several days for highly Alfvénic streams, but only for a few hours for ICMEs, leading to a considerably larger total amount of cross helicity in HSS related streams than in ICME-related solar wind.

The change in solar wind structure and the increase in the amount of Alfvénic fluctuations in 2003 coincide with the increase of substorm frequency by about 40%. Periodic southward intervals typical of highly Alfvénic solar wind produce repeated substorm intervals. Year 2003 marks the maximum occurrence of both storms and substorms, but the distribution of storms and substorms over the solar cycle is clearly different. A large majority of storms occurred before 2003 but most substorms thereafter. The annual number of substorms follows fairly reliably the evolution of the mean annual cross helicity. Our results suggest that the role of Alfvénic fluctuations in modulating substorm activity is large. Accordingly, the predictability of substorm frequency

and size would be greatly improved by monitoring the solar wind Alfvénic fluctuations in addition to the average values of the important solar wind parameters such as magnetic field and speed.

Acknowledgments

We wish to thank the institutes maintaining the IMAGE magnetometer network. The IMAGE magnetic field measurements are available via <http://space.fmi.fi/image/beta/> and auroral substorm and storm lists via <http://www.substormzoo.org>. The sunspot data were archived through SIDC-team, World Data Center for the Sunspot Index, Royal Observatory of Belgium, and interplanetary measurements via CDAWeb archive. The ICMEs are taken from the <http://www.srl.caltech.edu/ACE/ASC/DATA/level3/icmetable2.htm>, which is a catalogue by Richardson and Cane, and from the ACE ICME catalogue at <http://www.srl.caltech.edu/ACE/ASC/>. We acknowledge the financial support by the Academy of Finland to the ReSoLVE Centre of Excellence (project 272157) and by the European Community's Seventh Framework Program under grants 313038/STORM and 283676/ESPAS. M.K. acknowledges funding from the "Active Suns" research project of Helsinki University. We thank D.A. Roberts and A.J. Tanskanen for inspiring and constructive comments.

References

- Akasofu, S.-I., & Chapman, S. (1961). The ring current, geomagnetic disturbance, and Van Allen radiation belts. *Planetary and Space Science*, 66, 1321.
- Alfvén, H. (1942). Existence of electromagnetic-hydrodynamic waves. *Nature*, 150, 405.
- Banerjee, D., Pérez-Suárez, D., & Doyle, J. G. (2009). Signatures of Alfvén waves in the polar coronal holes as seen by EIS/Hinode. *Astronomy and Astrophysics*, 501, L15–L18.
- Belcher, J. W., & Davis, J. R. (1971). Large-amplitude Alfvén waves in the interplanetary medium, 2. *Journal of Geophysical Research*, 76, 3534–3563.
- Birkeland, K. (1908). *The Norwegian Aurora Polar Expedition 1902–1903* [vol. 1, 1st sect.]. Aschhoug, Oslo, Norway.
- Brier, G. W., & Bradley, D. A. (1964). The lunar synodical period and precipitation in the United States. *Journal of the Atmospheric Sciences*, 21, 386–395.
- Burlaga, L. F., Klein, L., Sheeley, N. R. Jr., Michels, D. J., Howard, R. A., Koomen, M. J., ... Rosenbauer, H. (1982). A magnetic cloud and a coronal mass ejection. *Geophysical Research Letters*, 12, 1317–1320. <https://doi.org/10.1029/GL009i012p01317>
- Cane, H. V., & Richardson, I. G. (2003). Interplanetary coronal mass ejections in the near-Earth solar wind during 1996–2002. *Geophysical Research Letters*, 108 (A4), 1156. <https://doi.org/10.1029/2002JA009817>
- Carrington, R. (1859). Description of a singular appearance seen in the Sun on September 1, 1859. *Monthly Notices of the Royal Astronomical Society*, 20, 13–15.
- Chapman, S., & Ferraro, V. C. A. (1930). A new theory of magnetic storms. *Nature*, 129, 3,169.
- Chian, A. C.-L., Kamide, Y., Rempel, E. L., & Santana, W. M. (2006). On the chaotic nature of solar-terrestrial environment: Interplanetary Alfvén intermittency. *Journal of Geophysical Research*, 111, A07S03. <https://doi.org/10.1029/2005JA011396>
- Chree, C. (1912). *Studies in Terrestrial Magnetism*, 206. London and New York: Macmillan.
- Coleman, P. J., Jr. (1968). Turbulence, viscosity, and dissipation in the solar-wind plasma. *The Astrophysical Journal*, 153, 371.
- Cummings, W. D., O'Sullivan, R. J., & Coleman, P. J., Jr. (1969). Standing Alfvén waves in the magnetosphere. *Journal of Geophysical Research*, 74, 778–793. <https://doi.org/10.1029/JA074i003p00778>
- D'Amicis, E., & Bruno, R. (2015). On the origin of highly Alfvénic slow solar wind. *The Astrophysical Journal*, 805, 84.
- D'Amicis, E., Bruno, R., & Bavassaro, B. (2011). Response of the geomagnetic activity to solar wind turbulence during solar cycle 23. *Journal of Atmospheric and Solar - Terrestrial Physics*, 83(5–6), 653. <https://doi.org/10.1016/j.jastp.2011.01.012>
- D'Amicis, R., Bruno, R., & Bavassano, B. (2007). Is geomagnetic activity driven by solar wind turbulence. *Geophysical Research Letters*, 34, L05108V. <https://doi.org/10.1029/2006GL028896>
- D'Amicis, R., Bruno, R., Bavassano, B., Carbone, V., & Sorriso-Valvo, L. (2006). On the scaling of waiting-time distributions of the negative IMF B_z component. *Annales de Geophysique*, 24(10), 2,735.
- Fairfield, D. H., & Cahill, L. J. Jr. (1966). Transition region magnetic field and polar magnetic disturbances. *Journal of Geophysical Research*, 71, 155–169. <https://doi.org/10.1029/JZ071i001p00155>
- Gonzalez, W. D., Clúa de Gonzalez, A. L., & Tsurutani, B. T. (1995). Geomagnetic response to large-amplitude interplanetary Alfvén wave trains. *Physica Scripta*, 55, 140–143.
- Häkkinen, L. V. T., Pulkkinen, T. I., Pirjola, R. J., Nevanlinna, H., Tanskanen, E. I., & Turner, N. E. (2003). Seasonal and diurnal variation of geomagnetic activity: Revised Dst versus external drivers. *Journal of Geophysical Research*, 108(A2), 1060. <https://doi.org/10.1029/2002JA009428>
- Holappa, L., Mursula, K., & Asikainen, T. (2014). A new method to estimate annual solar wind parameters and contributions of different solar wind structures to geomagnetic activity. *Journal of Geophysical Research*, 119, 9407–9418. <https://doi.org/10.1002/2014JA020599>
- Holappa, L., Mursula, K., Asikainen, T., & Richardson, I. G. (2014). Annual fraction of high-speed streams from principal component analysis of local geomagnetic activity. *Journal of Geophysical Research*, 119, 4544–4555. <https://doi.org/10.1002/2014JA019958>
- Holzer, R. E., & Slavin, J. A. (1981). The effect of solar wind structure on magnetospheric energy supply during solar cycle 20. *Journal of Geophysical Research*, 86, 675–680. <https://doi.org/10.1029/JA086iA02p00675>
- Hsu, T.-S., & McPherron, R. L. (2002). An evaluation of the sunsets. *Journal of Geophysical Research*, 107(A11), 1398. <https://doi.org/10.1029/2000JA000125>
- Kallio, E. I., Pulkkinen, T. I., Koskinen, H. E. J., Viljanen, A., Slavin, J. A., & Ogilvie, K. (2000). Loading-unloading processes in the nightside ionosphere. *Geophysical Research Letters*, 27, 1627–1630. <https://doi.org/10.1029/1999GL003694>
- Kilpua, K. E. J., Jian, L. K., Li, Y., Luhmann, J. G., & Russell, C. T. (2012). Observations of ICMEs and ICME-like solar wind structures from 2007–2010 using near-Earth and STEREO observations. *Solar Physics*, 281, 391–409.
- King, J., & Papitashvili, N. (2005). Solar wind spatial scales in and comparisons of hourly wind and ACE plasma and magnetic field data. *Journal of Geophysical Research*, 110, A02104. <https://doi.org/10.1029/2004JA010649>
- Kullen, A., & Karlsson, T. (2004). On the relation between solar wind, pseudobreakups and substorms. *Journal of Geophysical Research*, 109, A12218. <https://doi.org/10.1029/2004JA010488>
- Lee, D.-Y., Lyons, L. R., Kim, K. C., Baek, J.-H., Weygand, J., Moon, Y.-J., ... Han, W. (2006). Repetitive substorms caused by Alfvénic waves of the interplanetary magnetic field during high-speed solar wind streams. *Journal of Geophysical Research*, 111, A12214. <https://doi.org/10.1029/2006JA011685>
- Lepping, R. P., Acuña, M. H., Burlaga, L. F., Farrell, W. M., Slavin, J. A., Schatten, K. H., ... Worley, E. M. (1995). The wind magnetic field investigation. *Space Science Reviews*, 71, 207–229. <https://doi.org/10.1007/BF00751330>
- McComas, D., Bame, S., Barker, P., Feldman, W., Phillips, J., Riley, P., & Griffiee, J. (1998). Solar wind electron proton alpha monitor (SWEPAM) for the advanced composition explorer. *Space Science Reviews*, 86, 563–612. <https://doi.org/10.1023/A:1005040232597>
- McIntosh, S. W., De Pontieu, B., Carlsson, M., Hansteen, V., Boerner, P., & Goossens, M. (2011). Alfvénic waves with sufficient energy to power the quiet solar corona and fast solar wind. *Nature*, 475, 7357. <https://doi.org/10.1038/nature10235>
- McPherron, R. L., Weygand, J. M., & Hsu, T.-S. (2008). Response of the Earth's magnetosphere to changes in the solar wind. *Journal of Atmospheric and Solar - Terrestrial Physics*, 70, 303–315.
- Mursula, K., Holappa, L., & Lukianova, R. (2017). Seasonal solar wind speeds for the last 100 years: Unique coronal hole structure during the peak and demise of the Grand Modern Maximum. *Geophysical Research Letters*, 44, 30–36. <https://doi.org/10.1002/2016GL071573>

- Mursula, K., Lukianova, R., & Holappa, L. (2015). Occurrence of high-speed solar wind streams over the Grand Modern Maximum. *The Astrophysical Journal*, 801, 30. <https://doi.org/10.1088/0004-637X/801/1/30>
- Ogilvie, K. W., Chornay, D. J., Fritzenreiter, R. J., Hunsaker, F., Keller, J., Lobell, J., ... Gergin, E. (1995). SWE, a comprehensive plasma instrument for the wind spacecraft. *Space Science Reviews*, 71, 55–77. <https://doi.org/10.1007/BF00751326>
- Richardson, I. G., & Cane, H. V. (2012). Solar wind drivers of geomagnetic storms during more than four solar cycles. *Journal Space Weather Space Climate*, 2.(A01), 9. <https://doi.org/10.1051/swsc/2012001>
- Roberts, D. A., & Goldstein, M. (1990). Do interplanetary Alfvén waves cause auroral activity? *Journal of Geophysical Research*, 95(A4), 4327–4331. <https://doi.org/10.1029/JA095iA04p04327>
- Roberts, D. A., Goldstein, M. L., Klein, L. W., & Matthaeus, W. H. (1987). The nature and evolution of magnetohydrodynamic fluctuations in the solar wind: Voyager observations. *Journal of Geophysical Research*, 92, 12,023–12,035. <https://doi.org/10.1029/JA092iA10p11021>
- Sawyer, C., & Haurwitz, M. (1976). Geomagnetic activity at the passage of high-speed streams in the solar wind. *Journal of Geophysical Research*, 81(13), 2435–2436. <https://doi.org/10.1029/JA081i013p02435>
- Snekvik, K., Tanskanen, E. I., & Kilpua, K. E. J. (2013). An automated identification method for Alfvénic streams and their geoeffectiveness. *Journal of Geophysical Research*, 118, 1–13. <https://doi.org/10.1002/jgra.50588>
- Søråas, F., Aarsnes, K., Oksavik, K., Sandanger, M. I., Evans, D. S., & Greer, M. S. (2004). Evidence for particle injection as the cause of Dst reduction during HILDCAA events. *Journal of Atmospheric and Solar - Terrestrial Physics*, 66(2), 177.
- Sugiura, M. (1964). Hourly values of equatorial Dst for the IGY. *International Geophysical Year*, 35, 49.
- Tanskanen, E. I. (2009). A comprehensive high-throughput analysis of substorms observed by IMAGE magnetometer network: Years 1993–2003 examined. *Journal of Geophysical Research*, 114, A05204. <https://doi.org/10.1029/2008JA013682>
- Tanskanen, E. I., Pulkkinen, T. I., Viljanen, A., Mursula, K., Partamies, N., & Slavin, J. A. (2011). From space weather toward space climate time scales: Substorm analysis from 1993 to 2008. *Journal of Geophysical Research*, 116, A00143. <https://doi.org/10.1029/2010JA015788>
- Tanskanen, E. I., Pulkkinen, T. I., Koskinen, H. E. J., & Slavin, J. A. (2002). Substorm energy budget during low and high solar activity: 1997 and 1999 compare. *Journal of Geophysical Research*, 107(A6), 1086. <https://doi.org/10.1029/2001JA900153>
- Tanskanen, E. I., Slavin, J. A., Tanskanen, A. J., Viljanen, A., Pulkkinen, T. I., Koskinen, H. E. J., ... Eastwood, J. (2005). Magnetospheric substorms are strongly modulated by interplanetary high-speed streams. *Geophysical Research Letters*, 32, L16104. <https://doi.org/10.1029/2005GL023318>
- Tsurutani, B., Gonzalez, W. D., Gonzalez, A. L. C., Tang, F., Arballo, J. K., & Okada, M. (1995). Interplanetary origin of geomagnetic activity in declining phase of the solar cycles. *Journal of Geophysical Research*, 100(A11), 21,717–21,733. <https://doi.org/10.1029/95JA01476>
- Tsurutani, B. T., & Gonzalez, W. D. (1987). The cause of high-intensity long-duration continuous AE activity (HILDCAAs): Interplanetary Alfvén wave trains. *Planetary and Space Science*, 35(4), 405–412.
- Tsurutani, B. T., Gould, T., Goldstein, B. E., Gonzalez, W. D., & Sugiura, M. (1990). Interplanetary Alfvén waves and auroral (substorm) activity: IMP 8. *Journal of Geophysical Research*, 95, 2241. <https://doi.org/10.1029/JA095iA03p02241>
- Tu, C. Y., & Marsch, E. (1995). MHD structures, waves and turbulence in the solar wind: Observations and theories. *Space Science Reviews*, 73, 1–210. <https://doi.org/10.1007/BF00748891>
- Yakovchouk, O. S., Mursula, K., Holappa, L., Veselovsky, I. S., & Karinen, A. (2012). Average properties of geomagnetic storms in 1932–2009. *Journal of Geophysical Research*, 117(A3), A03201. <https://doi.org/10.1029/2011JA017093>
- Zhang, J., Richardson, I. G., Richardson, G., Webb, D. F., Gopalswamy, N., Huttunen, E., ... Zhukov, A. N. (2007). Solar and interplanetary sources of major geomagnetic storms ($Dst \leq 100$ nT) during 1996–2005. *Journal of Geophysical Research*, 112, A10102. <https://doi.org/10.1029/2007JA012321>